ENGINEERING JOURNAL

Article

Evaluation of Seismic Shear Demands of RC Core Walls in Thailand Determined by RSA Procedure

Kimleng Khy[a] **and Chatpan Chintanapakdee**[b,*]

Center of Excellence in Earthquake Engineering and Vibration, Department of Civil Engineering, Faculty of Engineering, Chulalongkorn University, Bangkok 10330, Thailand
E-mail: [a]khy_kimleng@yahoo.com, [b]chatpan.c@chula.ac.th (Corresponding author)

Abstract. ASCE 7 allows structural engineers to use Response Spectrum Analysis (RSA) procedure to compute the seismic design forces of the structures. However, seismic shear demands of reinforced concrete (RC) walls determined by RSA have been found to be inadequate by many researchers. This paper aims to investigate the seismic shear demands of RC core walls from low-rise to high-rise buildings. RC split core walls in five buildings varying from 5 to 25 stories subjected to earthquake ground motions in Bangkok and Chiang Mai of Thailand were first designed by RSA procedure in ASCE 7-10. Then nonlinear response history analysis (NLRHA) was conducted to compute more accurate seismic demands of the structures. The results demonstrated that shear demands of core walls from NLRHA were significantly larger than those from RSA procedure. The shear amplifications of core walls in cantilever-wall direction were larger than those in coupled-wall direction. The two building locations having different spectrum shapes led to different shear amplifications. Hence, an empirical formula cannot be applied to every location. In Bangkok, it is found that Rejec et al. (2012)'s equation could well estimate shear forces in cantilever direction of core walls but it significantly overestimated shear forces in coupled direction of core walls. In Chiang Mai, Luu et al. (2014)'s equation provided good estimation of shear forces in both directions of core walls. Beside these two equations, the shear magnification factor equation in EC8 is found acceptable to be adopted to multiply with shear force from RSA procedure before using it as design shear force of RC core wall in both Bangkok and Chiang Mai.

Keywords: Seismic shear demand, reinforced concrete core wall, response spectrum analysis, nonlinear response history analysis.

ENGINEERING JOURNAL Volume 21 Issue 2
Received 19 June 2016
Accepted 19 August 2016
Published 31 March 2017
Online at http://www.engj.org/
DOI:10.4186/ej.2017.21.2.151

DOI:10.4186/ej.2017.21.2.151

1. Introduction

Reinforced concrete (RC) core walls are extensively used as seismic force resisting systems. To design such buildings under earthquake loading, engineers in Thailand usually employ modal response spectrum analysis (RSA) procedure in ASCE 7-10 [1] to determine the design forces of the walls. The design forces in this method are obtained by using a single response modification factor (R) for all modes of response to reduce the elastic forces computed by RSA procedure. However, previous researchers have found that flexural yielding at the base region of the wall reduced mainly the first-mode shear but higher-mode shears were not significantly affected by inelastic action [2-5]. Most studies were based on comparing results from RSA procedure to the 'referenced' results from nonlinear response history analysis (NLRHA), which is considered as the most accurate method available to compute design forces of a structural system subjected to earthquake loading. However, NLRHA is too complicated and time-consuming for practical design. When flexural capacity at the base of the wall was reached, the flexural over-strength inherent in the design could increase shear force of the wall. This increase was predominately related to the first-mode shear response [6]. ASCE 7-10 uses the same R for reducing shear force and bending moment expecting that flexural yielding at the base region of the wall limits shear force in the same way as it limits bending moment of the wall. NLRHA results show that shear force keeps increasing after flexural yielding occurred at the base of the wall. The ratio between shear force from NLRHA and from RSA procedure is regarded as shear amplification. Therefore, when contribution of higher modes is significant and flexural over-strength of the wall is large, RSA procedure leads to non-conservative estimation of shear demands in nonlinear RC walls.

Consequently, some seismic design codes, National Building Code of Canada (NBCC) [7] ,Canadian Standard Association (CSA A23.3) [8]; Eurocode 8 (EC8) [9] and New Zealand Standard (NZS 3101) [10] have already been modified to account for shear amplification of structural wall, but there is no such shear amplification in ASCE 7-10 yet based on Rutenberg [11]. Regarding to this problem, it should be kept in mind that United States commonly design tall buildings by using NLRHA at the Risk-Targeted Maximum Considered Earthquake (MCE_R) level of ground motion which consumes much effort and time to conduct the analysis. However, Thailand adopting mostly the ASCE 7-10 still uses RSA procedure to determine the design shear force for RC wall which can lead to unsafe result. A case study of 16-story building in Bangkok conducted by Leng et al. [12] confirmed that the base shear and bending moment demands from NLRHA were approximately 2.5 and 2 times, respectively, the demands from RSA procedure.

Although, previous researchers have studied higher-mode shear in RC wall, most of them have mainly focused on RC cantilever wall designed for a concentrated plastic hinge at the base of the wall. None of these studies focused on split core-wall systems which are widely constructed in Thailand. Thus, this study attempts to investigate the shear demands in such systems and aims to explore the accuracy of various codes and previous researchers' formulas if applied to the core-wall structures.

2. Review on Higher-Mode Shear Demands in RC Wall

Shear amplification in RC wall has been recognized since 1975 and was firstly studied by Blakeley et al. [13]. Many subsequent studies have mainly focused on the estimation of shear forces in RC cantilever wall designed for a single plastic hinge at the base. Several equations for estimating shear forces in RC cantilever wall, particularly the base shear forces, have been developed based on their parametric studies such as structural configurations and ground motions. Obviously, the results depend on these choices.

NZS 3101 [10] outlines that the design shear force of the wall shall not be less than the shear force determined by multiplying the shear force from equivalent static analysis, V_E, with base shear amplification factor, ω_v, proposed by Blakeley et al. [13], and flexural over-strength factor, ϕ_o.

$$V_o^* = \omega_v \phi_o V_E \tag{1}$$

$$\omega_v = \begin{cases} 0.9 + \dfrac{n}{10} & \text{for n} \le 6 \\ 1.3 + \dfrac{n}{30} \le 1.8 & \text{for n} > 6 \end{cases}$$

where V_o^* is the design shear force at any level of the wall, ϕ_o is the over-strength factor related to flexural action at any level of the wall and *n* is number of stories of the building.

The design shear force of RC wall, V_{Ed}, in EC8 [9] is computed by amplifying shear force, $V_{Ed}^{'}$, obtained from RSA with a shear magnification factor, ε. The value of ε is taken as 1.5 for moderately ductile wall (*q*<3). For highly ductile wall, it is calculated from Eq. (2), which was based on formula proposed by Eibl and Keintzel [3]. The value of ε has to be at least 1.5, but needs not be larger than *q*. EC8 uses ε as a constant factor along the height of the wall.

$$V_{Ed} = \varepsilon V_{Ed}^{'}$$
$$\varepsilon = q\sqrt{\left(\frac{\gamma_{Rd}}{q}\frac{M_{Rd}}{M_{Ed}}\right)^2 + 0.1\left(\frac{S_e(T_C)}{S_e(T_1)}\right)^2} \quad (2)$$

where ε is the base shear magnification factor, q is the behavior factor (force reduction factor used in design), M_{Rd} is the design flexural strength at the base of the wall, M_{Ed} is the design bending moment obtained from RSA at the base of the wall, γ_{Rd} is the over-strength factor accounting for strain-hardening of rebar, T_c is the upper-limit period of constant spectral acceleration region, T_1 is the fundamental period of building in the direction of shear force considered and $S_e(T)$ is ordinate of the elastic response spectrum.

Rutenberg and Nsieri [14] indicated that shear magnification equation in EC8 as defined here by Eq. (2) could significantly overestimate the base shear force in short period ductile wall while underestimate it for long period one. In an attempt to improve the estimation, they proposed the following formulas to determine the design base shear force of RC cantilever wall.

$$V_a = \omega_v^* V_d = \left[0.75 + 0.22\left(T + q + Tq\right)\right]V_d \quad (3)$$

$$V_d = \frac{M_y}{(2/3)H\left[1 + (1/2n)\right]} \quad (4)$$

where ω_v^* is the base shear amplification factor, V_d is the base shear causing flexural yielding, M_y, at the base of the wall, *q* is behavior factor, *H* is the building height and *n* is the number of stories. They further proposed a tri-linear design shear envelop (Fig. 1(a)) as a function of the fundamental period, *T*, and ξ defined by Eq. (5) to estimate design shear force along the height of the wall.

$$\xi = 1.0 - 0.3T \geq 0.5 \quad (5)$$

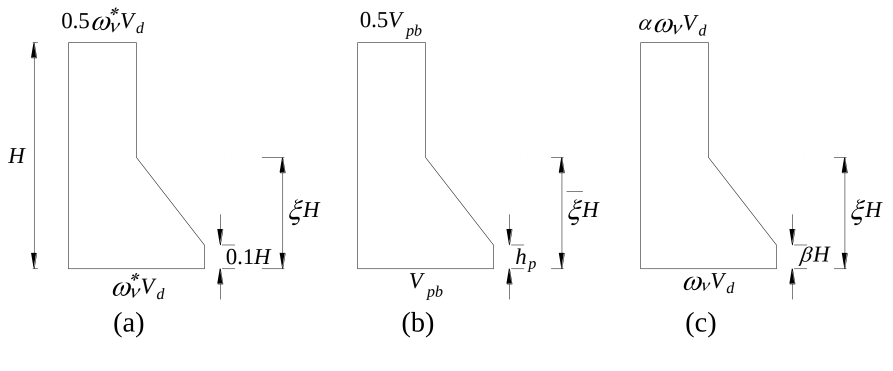

Fig. 1. Design shear envelop proposed by (a) Rutenberg and Nsieri [14]; (b) Boivin and Paultre [15]; and (c) Luu et al. [16].

DOI:10.4186/ej.2017.21.2.151

Another study was conducted by Rejec et al. [6] to propose possible improvement to Eq. (2). They found that the design shear force in EC8 should be computed from the first-mode shear, $V'_{Ed,1}$, amplified by the magnification factor, ε_a. The factor, ε_a, in their proposed formula was derived in the same manner as EC8's equation but they did not limit ε_a by factor, q. They limited the base shear force of the wall by elastic shear force as included in the first term of ε_a. So, they modified Eq. (2) as:

$$V_{Ed,a} = \varepsilon_a V'_{Ed,1}$$
$$\varepsilon_a = q\sqrt{\left(\min\left[\frac{\gamma_{Rd}}{q}\frac{M_{Rd}}{M_{Ed}};1\right]\right)^2 + 0.1\left(\frac{S_e(T_C)}{S_e(T_1)}\right)^2} \geq 1.5 \tag{6}$$

Eq. (6) was applicable only to the base shear force of RC cantilever wall. They further proposed formula to compute the shear force along the height of the wall by replacing the constant 0.1 with the ratio between static response contribution of second mode and that of the first mode which varies along the height of the wall, $m(z)$, as shown in Eq. (7).

$$\varepsilon_a(z) = q\sqrt{\left(\min\left[\frac{\gamma_{Rd}}{q}\frac{M_{Rd}}{M_{Ed}};1\right]\right)^2 + m(z)^2\left(\frac{S_e(T_C)}{S_e(T_1)}\right)^2} \geq 1.5 \tag{7}$$

where z is the vertical coordinate of the wall.

Priestley [5] proposed Modified Modal Superposition (MMS) approach to determine the design shear force for RC cantilever wall, as shown in Eq. (8). This method was developed based on the assumption that inelastic action only limited the shear force from the first mode and shear force from higher modes were not affected by inelastic action.

$$V_i = \left(V_{1i}^2 + V_{2Ei}^2 + V_{3Ei}^2 + \ldots\right)^{0.5} \tag{8}$$

where V_i is the design shear force of the wall at level i, V_{1i} is the lesser of elastic first-mode and ductile first-mode shear computed by direct displacement base design (DDBD) at level i, V_{2Ei} and V_{3Ei} are elastic modal shear at level i for second and third mode, respectively.

NBCC [7] has explicitly considered higher-mode effects when using equivalent static force procedure by applying higher-mode factor, M_v, to increase the base shear force and by applying base overturning reduction factor, J, to reduce overturning moment. These factors depend on the structural type, fundamental period of the structure and the shape of design spectrum. In addition to NBCC [7], CSA A23.3 [8] contains specific provisions for seismic design of shear wall. For ductile wall, it requires that the base shear resistance must be increased by the ratio of base probable bending moment capacity to the base bending moment obtained from RSA, which is actually the base flexural over-strength of the wall. For moderately ductile wall, the same calculation is followed by using base nominal bending moment capacity instead of base probable bending moment capacity. Based on Adebar et al. [17], the new provision of CSA A23.3 requires that the design shear force of the wall shall not be greater than elastic shear force from RSA reduced by force reduction factor equal to 1.3.

Boivin and Paultre [15] proposed capacity design method for shear strength design of regular ductile RC cantilever wall for CSA A23.3 [8]. Their proposed method was based on a parametric study of ductile walls subjected to Western North America ground motions. They stated that base shear force was primarily influenced by wall over-strength factor and fundamental period. A new base shear amplification factor value, $\bar{\omega}_v$, was proposed as indicated in Table 1. The design base shear force, V_{pb}, was calculated by Eq. (9).

$$V_{pb} = \bar{\omega}_v V_{Pbase} \leq V_{\text{base,limit}}$$
$$V_{Pbase} = V_f\left(\frac{M_p}{M_f}\right)_{\text{base}} \tag{9}$$

Table 1. Proposed base shear amplification factor value, $\bar{\omega}_v$, by Boivin and Paultre [15].

$R_d R_o / \gamma_w$	$T_1 \le 0.5$	$T_1 \ge 1.0$
2.80	1.0	2.0
1.87	1.0	1.5
≤ 1.40	1.0	1.0

where V_{Pbase} is the probable shear force at the base of the wall as required by CSA A23.3 [8], $V_{\text{base,limit}}$ is the base share force limit as required by the code, V_f and M_f are the design base shear force and base bending moment obtained from RSA, respectively, and M_p is the base probable moment capacity of the wall.

Boivin and Paultre [15] also recommended using the tri-linear design shear envelop (Fig. 1(b)) modified from [14], with a new equation for $\bar{\xi}$ as shown in Eq. (10).

$$\bar{\xi} = 1.5 - T_1; \quad 0.5 \le \bar{\xi} \le 1 \tag{10}$$

Luu et al. [16] performed a parametric study to examine the seismic demands of moderately ductile (MD) RC shear walls subjected to high-frequency Eastern North America earthquakes. A new base shear amplification factor, ω_v, applied to the base shear, V_d, obtained from RSA was proposed for NBCC [7] and CSA A23.3 [8] for MD shear walls.

$$V_b = \omega_v V_d \tag{11}$$
$$\omega_v = \begin{cases} 1.6 + 0.7(\gamma_w - 1) + 0.2(T - 0.5) & \text{if } 0.5 \le T \le 1.5 \text{ sec} \\ 1.8 + 0.7(\gamma_w - 1) - 0.1(T - 1.5) & \text{if } 1.5 < T \le 3.5 \text{ sec} \end{cases}$$

where V_b is the design base shear force of the wall, T is the fundamental period and γ_w is the base flexural over-strength factor of the wall.

Shear force design envelop similar to [14] was also proposed by [16] with few modification as presented in Eq. (12). These parameters could be clearly seen in design shear envelop in Fig. 1(c).

$$\xi = 1.2 - 0.4T \quad 0.6 \le \xi \le 1 \tag{12}$$
$$\alpha = 0.4\,;\ \beta = 1/n$$

3. Methodology

The procedure to conduct this study is outlined as the followings:

- Review the background of various codes and previously proposed formulas for estimating the seismic shear demands of RC shear walls.
- Select the common structural parameters to be studied.
- Analyse the structures by RSA procedure using ETABS program [18], then determine the seismic demands.
- Design the structural systems such that the nominal strength multiplied by the corresponding strength reduction factor in accordance with ACI 318-11 [19] is approximately equal to the factored demands obtained from RSA procedure.
- Analyse the structures already designed with internal forces computed from RSA procedure by NLRHA using PERFORM-3D program [20].
- Compare the results from NLRHA with those from RSA procedure.
- Evaluate the accuracy of various codes and previously proposed formulas for estimating shear demand of RC wall.
- Recommend appropriate modification of RSA procedure in design of RC core wall.

DOI:10.4186/ej.2017.21.2.151

3.1. Structural Systems

This study used five RC split core-wall buildings ranging from 5- to 25-story having core walls located at the center of a square-shape floor plan. The orientation of core-wall cross section of each building was presented in Fig. 2. Each building consists of two core walls coupled by coupling beams (long coupling beams, LCB) in X direction with the exception that 5-story building has only one central core wall. The openings for elevator doors have short coupling beams (SCB) in Y direction above the openings. The building characteristics were presented in Table 2. Core walls were assumed to have uniform cross section throughout the height. The coupling beams in each direction were considered to have the same stiffness and strength over the entire height of each building. The concrete compressive strength used in this study slightly increases as number of stories increases because taller buildings usually utilize higher compressive strength of concrete. Varying concrete compressive strength is not expected to significantly influence accuracy of RSA procedure.

Table 2. Building characteristics.

No. of Story	H (m)	A_f (m²)	W_f (kN)	f_c' (MPa)	f_y (MPa)	t_w (m)	LCB (m²)	SCB (m²)	T_1 (sec)	
									X	Y
5	15	380	3,383	30	390	0.20	-	0.20 x 0.80	0.57	0.43
10	30	792	7,318	30	390	0.25	0.25 x 0.50	0.25 x 0.80	1.62	1.29
15	45	1,080	9,903	35	390	0.30	0.30 x 0.50	0.30 x 0.80	2.68	1.71
20	60	1,225	11,550	35	390	0.35	0.35 x 0.50	0.35 x 0.80	3.72	2.05
25	75	1,376	13,278	40	390	0.40	0.40 x 0.50	0.40 x 0.80	4.60	2.27

Notes: H is the building height, A_f is the floor area, W_f is the seismic weight per floor, f_c' is the compressive strength of concrete, f_y is the yield strength of rebar, t_w is the wall thickness, T_1 is the fundamental period of the building.

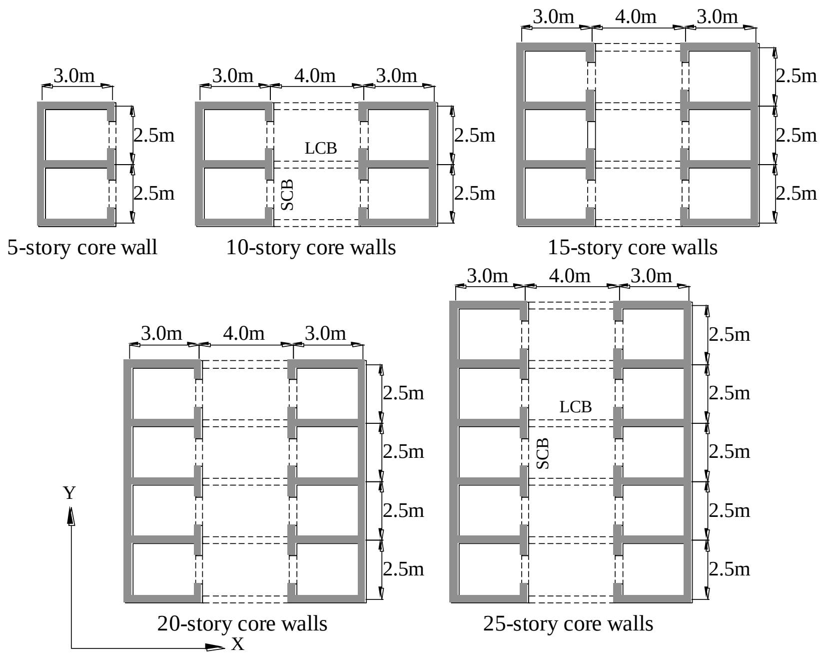

Fig. 2. Core-wall cross sections for the five studied buildings.

3.2. Modeling of Structural Systems

RC spilt core walls were designed to resist the entire lateral loads; hence, only the structural split core-wall systems were modeled by ignoring the stiffness and strength of the gravity columns and slabs. However, in nonlinear model, p-delta effects due to the gravity columns were included by creating a dummy column with no lateral stiffness at the center of each core wall and by slaving the column ends with other nodes at each floor, recommended by Powell [21]. Rigid diaphragm was assigned to the floor slab assuming that the floor was rigid in plane. Floor masses were computed from all dead loads and were assigned to the center of mass at each floor level. Foundation was assumed to be fixed support.

3.2.1. Linear modeling of structural systems

Linear structural model was created in ETABS program [18] for conducting RSA procedure. Wall was modeled by shell elements. Short coupling beam (SCB) was modeled by shell elements. Long coupling beam (LCB) was modeled as a frame element connected to the walls by an embedded rigid beam to ensure the rigid connection between the coupled walls and LCB. The effective stiffness values of the structural members given in ACI 318-11 were used to account for cracked sections of RC members as presented in Table 3.

3.2.2. Nonlinear modeling of structural systems

Nonlinear structural model was constructed in PERFORM-3D program [20] for conducting NLRHA. Core walls were modeled using inelastic fiber shear wall elements represented by the concrete and steel properties to capture axial-moment interaction behavior. The in-plane shear stiffness was modeled using elastic shear properties with reduced shear stiffness of $GA/10$ to account for shear cracking recommended by PEER/ATC-72-1 [22]. The material stress-stain relationships for confined and unconfined concrete proposed by Mander et al. [23] were adopted such that it was represented by a tri-linear relationship in PERFORM-3D program. The steel material was modeled with tri-linear stress-strain relationship with strain-hardening ratio of 3%. The ultimate strain of the steel was assumed to be 0.09 (=60% of value specified in Thai industrial standard as recommended by Priestley et al. [24]). Cyclic degradation parameters were taken from Moehle et al. [25]. Nonlinear fiber model was incorporated over the entire height of the core wall. In each core-wall cross section, the web consists of eight concrete fibers along with eight steel fibers while the flange consists of three concrete fibers and three steel fibers. Concrete fibers in the webs are modeled as confined concrete near the edges (smaller fibers) and unconfined concrete in the middle region (relatively large fibers), whereas concrete fibers in the flanges are all confined concrete. Steel fibers are distributed with uniform spacing for both webs and flanges, for simplicity. An example of core-wall fiber section of 5-story building was shown in Fig. 3.

Short coupling beams (SCB), span to depth ratio of 1.5, were modeled using a nonlinear shear displacement-hinge at the center of the beam with modeling parameters based on test results of Naish et al. [26]. The long coupling beams (LCB), span to depth ration of 8, included rotational plastic hinge elements at both ends. The coupling beams were connected to the walls using embedded rigid beam to ensure the rigid connection between the coupled walls and coupling beams. The effective elastic stiffness for bending of 0.20 EI_g is used for elastic portion to account for slip/extension deformations at beam-wall interface suggested by Naish et al. [26].

DOI:10.4186/ej.2017.21.2.151

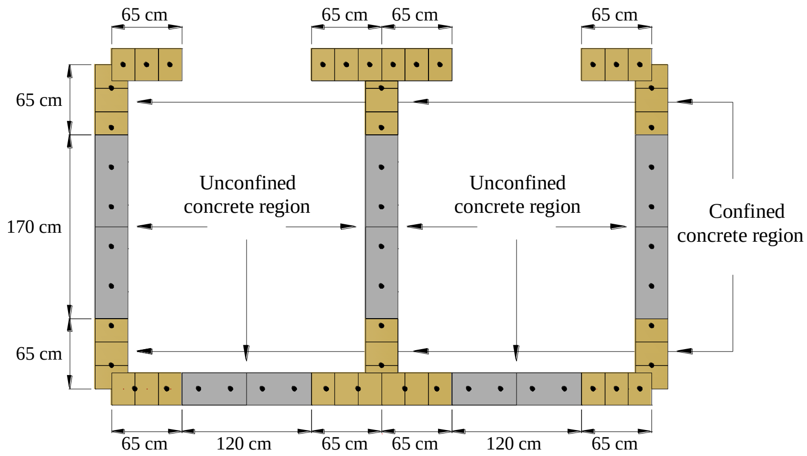

Fig. 3. Core wall fiber section of 5-story building.

Table 3. Effective stiffness of elastic structural members used in RSA and NLRHA.

Elements	**RSA**		**NLRHA**	
	Flexural	**Shear**	**Flexural**	**Shear**
Shear wall	0.70 EI_g	1.0 GA_g	Fiber section	0.1 GA_g
Coupling beam	0.35 EI_g	1.0 GA_g	0.20 EI_g	1.0 GA_g

3.3. Ground Motions

The maximum considered earthquake (MCE) ground motions having 2 percent probability of exceedance within 50 years were employed in this study. It should be noted that RSA procedure in ASCE 7-10 uses the design spectrum that is referred to design basic earthquake (DBE) ground motions having 10 percent probability of exceedance within 50 years. DBE is computed by multiplying MCE with a factor of 2/3. MCE is generally used in NLRHA to evaluate the response of the structural system against collapse. However, for Bangkok (low seismic zone), MCE was used for both RSA and NLRHA in this study because the structural systems did not yield much under DBE. For Chiang Mai (high seismic zone), DBE was employed for both RSA and NLRHA. Using the same intensity of ground motions for RSA and NLRHA is appropriate for the purpose of comparing analysis methods.

For Bangkok, a set of seven ground motions selected from PEER Ground Motion Database was used. They were modified and scaled such that their spectra matched the bed-rock target spectrum of Palasri and Ruangrassamee [27]. Then, those spectral-matching ground motions were input in ProShake program [28] to simulate the wave propagation through layers of soft soil in Bangkok. The resulted pseudo-acceleration response spectra with 5% damping ratio of soft-soil ground motions were plotted in Fig. 4.

For Chiang Mai, ten pairs of ground motions selected from PEER Ground Motion Database were employed. Those ground motions were multiplied by a factor such that mean SRSS spectrum of the ten pairs of ground motions was not less than 1.17 times the design spectrum per ASCE 7-10. The component with larger PGA was selected from each of the ten pairs to make a set of ten ground motions to be employed in NLRHA. The resulted pseudo-acceleration response spectra and the mean spectrum of these ten records were illustrated in Fig. 5.

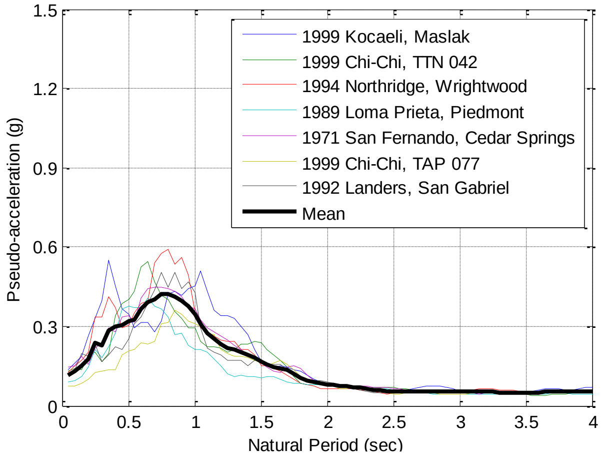

Fig. 4. Elastic response spectra and mean spectrum of 7 soft-soil ground motions for Bangkok.

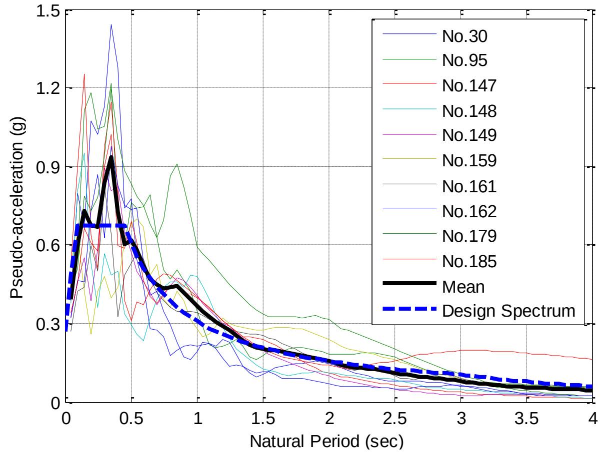

Fig. 5. Elastic response spectra, mean spectrum of 10 ground motions and the design spectrum for Chiang Mai.

4. Response Spectrum Analysis Procedure

4.1. Design and Analysis Considerations

The structures were designed such that their nominal strengths multiplied by the corresponding strength reduction factor in accordance with ACI 318-11 were approximately equal to the factored demands obtained from RSA procedure in ASCE 7-10. The lateral force resisting system was considered to be special RC shear wall whose design factors were: response modification factor (R=6), deflection amplification factor (C_d=5) and important factor (I=1.25). Wind load was not considered in this study. The seismic load was applied in each direction separately at a time. The vertical seismic load effect was not considered in this study. Basic load combinations for strength design in ASCE 7-10 as presented in Table 4 were considered. Constant modal damping ratio of 5% was employed.

Story drift in ASCE 7-10 is obtained from RSA procedure by scaling up with a factor of C_d/I after reducing the elastic spectrum by a factor of R/I. ASCE 7-10 requires that dynamic base shear (V_d) determined by RSA is at least equal to 85% of the static base shear (V_s) computed by equivalent lateral force (ELF) procedure. Such scaling results in effective response modification factor, R_{eff}, which is the ratio between elastic base shear and design base shear. The factor R_{eff} is computed by Eq. (13). The values of R_{eff} in each direction of all buildings were summarized in Table 5.

$$R_{eff} = \min\left(\frac{R}{I}\times\frac{V_d}{0.85V_s}, \frac{R}{I}\right) \tag{13}$$

Table 4. Load combinations used in RSA and NLRHA.

Analysis type	Load Combination
RSA	$1.2D+0.5L\pm Q_E$
	$0.9D\pm Q_E$
NLRHA	$1.0D+0.25L+Q_E$

D, L and Q_E are dead load, unreduced live load and earthquake load, respectively.

DOI:10.4186/ej.2017.21.2.151

Table 5. Effective response modification factor of structural systems.

No. of Story	Bangkok		Chiang Mai	
	$R_{eff,x}$	$R_{eff,y}$	$R_{eff,x}$	$R_{eff,y}$
5	3.68	4.02	3.87	3.93
10	2.91	3.70	4.44	4.73
15	3.52	4.00	4.23	4.80
20	4.09	3.96	2.94	4.80
25	3.48	3.82	2.49	4.80

4.2. Story Drift, Bending Moment and Shear Response Behavior

Figure 6 shows that as the structural heights increase, higher modes become more dominant for all responses, even though the mass participations of higher modes are smaller than that of the first mode. Only the results of 10-story and 25-story buildings subjected to mean spectrum of Bangkok in X direction are presented here. Similar trend is observed for design spectrum in Chiang Mai. The modal contributions to the total response are totally different between story drift, bending moment and shear response. For story drift, the first-mode contribution is always dominant along the height of the structure for all buildings. For bending moment, the first mode is dominant at the base of the structure for all buildings, while higher modes play an important role around mid-height for tall building (Fig. 6(b)). For shear, second-mode contribution is considerably significant at the base of the structure even for shorter buildings. For tall building, it is not appropriate to assume that bending moment and shear response display the same inelastic behavior by applying the same response modification factor because higher-mode response do not yield as much as the first-mode response.

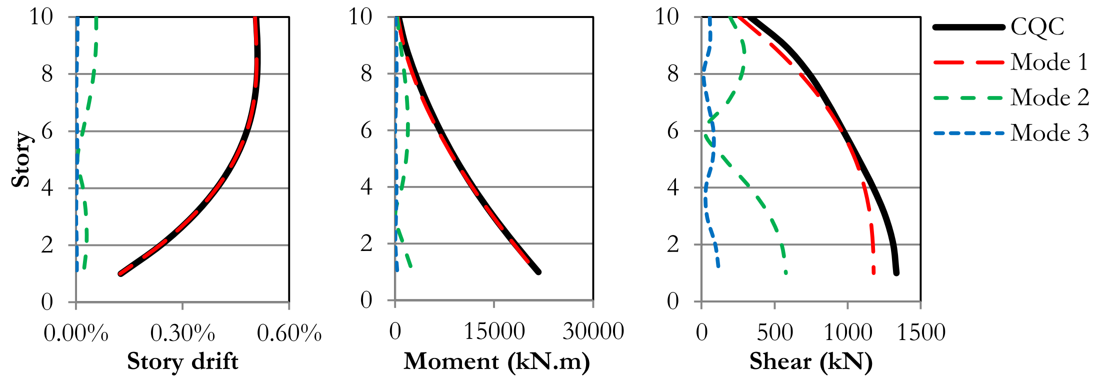

(a) 10-story core wall

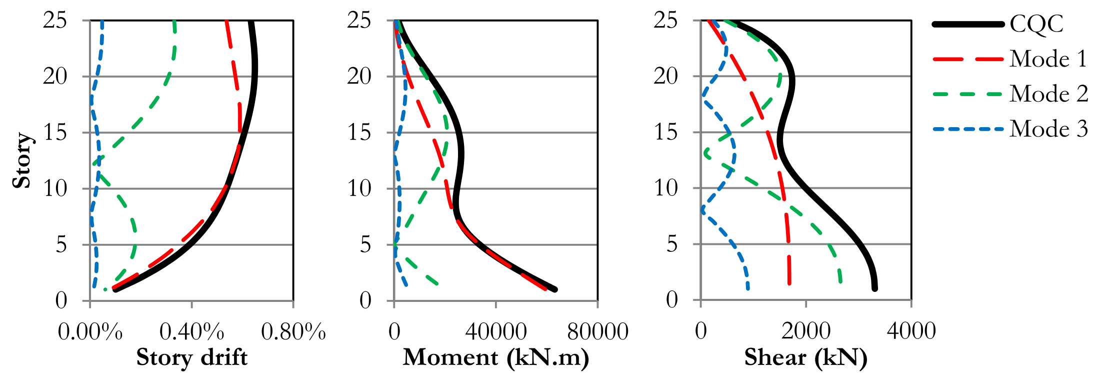

(b) 25-story core wall

Fig. 6. Story drift, bending moment and shear profiles contributed from the first-three modes and the combined peak response under earthquake in X direction: (a) 10-story; and (b) 25-story core walls.

DOI:10.4186/ej.2017.21.2.151

4.3. Base Moment and Base Shear Modal Contribution Ratio

The modal contribution ratio of each mode is defined here as:

$$\bar{F}_i = \frac{F_i}{F_{CQC}} \tag{14}$$

where $\bar{F}_i$ is the modal contribution ratio of response in mode i, F_i is the peak modal response of mode i, F_{CQC} is the combined peak response.

The variations of modal contribution ratio with fundamental period for base shear and base moment under earthquake in X direction of the five studied structures were presented both for Bangkok (BKK) and Chiang Mai (CM) in Fig. 7. For Bangkok, second-mode contribution overtook the first-mode contribution for periods longer than 2.2 seconds for base shear responses while base moment responses were always dominated by the first mode for all periods considered. For Chiang Mai, second-mode contribution was dominant for periods longer than 1.6 seconds for base shear responses, whereas base moment responses were observed the same thing as in Bangkok. From this investigation, it can be concluded that for the same structural systems subjected to ground motions having different spectrum shapes, higher-mode contributions for base shear are different.

Figure 7 highlights the fact that higher modes are the primary contributors to base shear for tall buildings with long fundamental periods. Note that these trends are not always the general case because they are derived from the five studied structures and spectral shapes considered in this study.

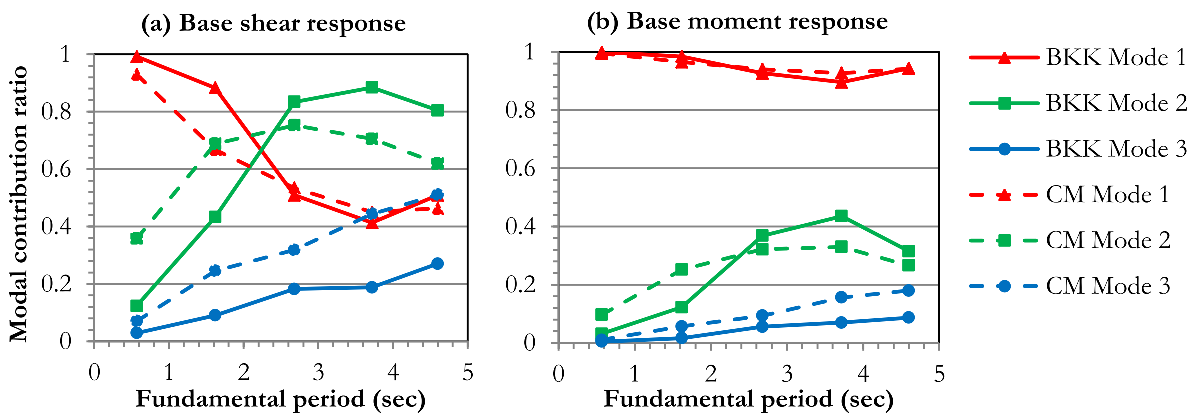

Fig. 7. Modal contribution ratios for the first-three modes under earthquake in X direction: (a) base shear response and (b) base moment response.

5. Nonlinear Response History Analysis

NLRHA was conducted by using PERFORM-3D program [20]. Rayleigh damping was implemented with 4% damping ratio (as recommended by PEER/ATC-72-1 [22]) specified in the first and third modes. The gravity load of D+0.25L was applied before running NLRHA. For Bangkok, seven ground motions were used while for Chiang Mai, ten ground motions were employed. The ground motions were applied in each direction separately at a time.

6. Comparison of Seismic Demands Computed by RSA Procedure and NLRHA

Base shear amplification (BSA) is defined as the ratio between shear force in a core wall from NLRHA and design shear force in RSA procedure. Base moment amplification (BMA) is defined as the ratio between bending moment in a core wall from NLRHA and design bending moment in RSA procedure. Base flexural over-strength (BFOS) is defined as the ratio between actual ultimate bending moment capacity of a core wall and design bending moment in RSA procedure. Bending moment strength of core wall is determined from P-M interaction diagram with the axial load of D+0.25L.

6.1. Base Shear and Base Moment Amplification of Core Wall

Figure 8 showed that base shear amplifications (BSA) were generally greater than two. The results in both locations, Bangkok and Chiang Mai, were significantly different under earthquake in Y direction (EQy) as shown in Fig. 8(b) where core walls behave like cantilever walls. In Y direction, BSAs were as large as five for 20- and 25-story buildings in Bangkok while in Chiang Mai, BSAs were relatively smaller and were about three for 10- to 25-story buildings. In X direction (Fig. 8(a)) where core walls behave like coupled walls, BSAs were smaller than in Y direction and BSAs in Bangkok were only slightly larger than in Chiang Mai. From detail investigation, it was found that core walls under earthquake load in X direction (EQx) did not yield much at the base while the coupling beams sustained wide spread yielding at several plastic hinges in the upper stories dissipating much energy. This may be the reason why core walls suffered little yielding and smaller shear amplification. The differences of BSA in both locations are primarily attributed to different base flexural over-strength (BFOS) of core wall (Fig. 9) and higher-mode contributions due to different spectrum shape as explained in Section 4.3. The sensitivity of BSA of core wall to BFOS of core wall will be investigated in Section 8.

Unlike base shear response, base moment response is contributed mainly from the first mode and the base moment is limited by actual flexural capacity of core wall which is dependent on axial load. Due to different axial load of core walls (D+0.25L for NLRHA and 0.9D, which governed the design, for RSA procedure) and flexural over-strength inherent in the design, bending moments in core walls from NLRHA were larger than those from RSA procedure (Fig. 10). As shown in Fig. 11, the bending moment demand of core wall from NLRHA was located at the actual P-M interaction surface and was larger than the design moment from RSA procedure. The design P-M interaction diagram is the actual P-M interaction diagram multiplied by strength reduction factor in ACI 318-11. In cantilever direction (Fig. 10(b)), base moment amplifications (BMA) could be as high as three in Bangkok and two in Chiang Mai. Whereas in coupled direction (Fig. 10(a)), BMA was relatively smaller than in cantilever direction. The difference of BMA and BFOS between the two directions of core wall came from the design process. In designing the vertical reinforcement of the core walls, the bending moment demands due to EQx and EQy were considered. The bending moment demands due to EQx governed the design for most of the buildings and resulted in smaller BFOS in X direction than in Y direction for those buildings.

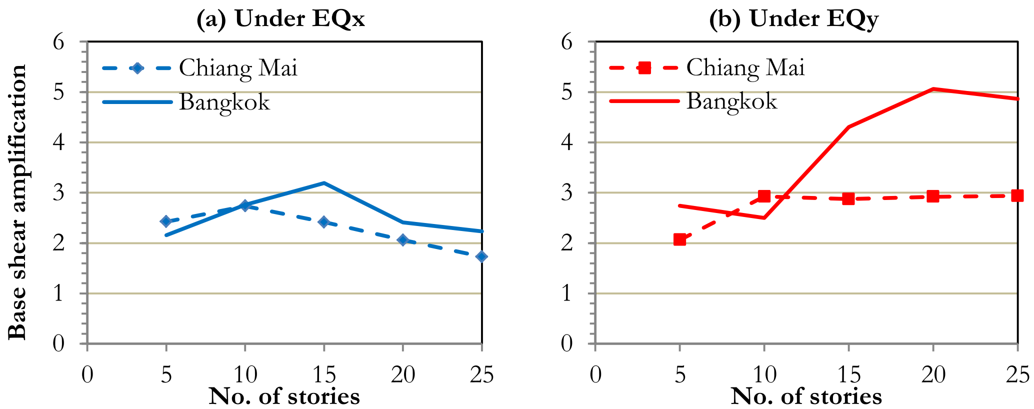

Fig. 8. Base shear amplifications of core wall: (a) under EQx; and (b) under EQy.

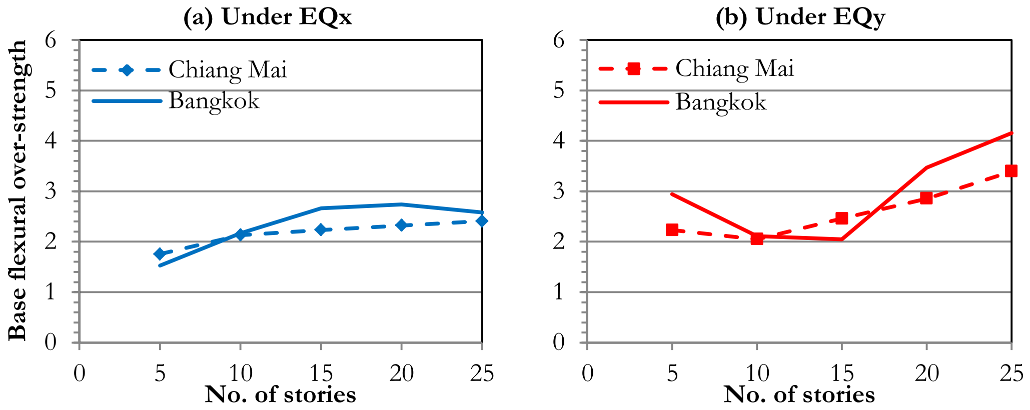

Fig. 9. Base flexural over-strengths of core wall: (a) under EQx; and (b) under EQy.

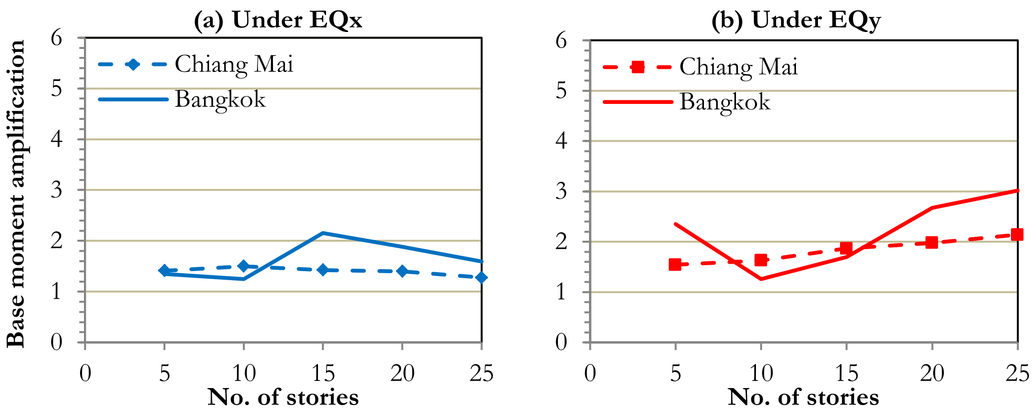

Fig. 10. Base moment amplifications of core wall: (a) under EQx; and (b) under EQy.

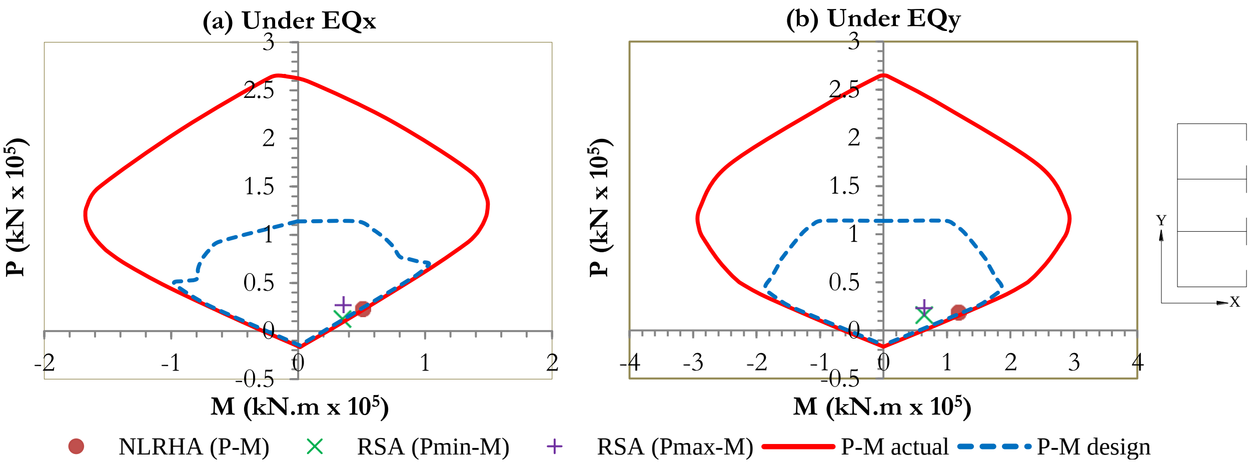

Fig. 11. Comparison of actual and design P-M interaction diagram of 15-story core wall in Chiang Mai: (a) under EQx; and (b) under EQy.

6.2. Shear, Bending Moment and Story Drift Along the Height of Structure

The core wall is utilized to resist lateral load in both X and Y directions. The stiffness in resisting earthquake in Y direction, which behaves as cantilever wall, is larger than in X direction, which behaves as coupled wall; thus for NLRHA, Y direction attracts more shear force ($V_{y,\mathrm{NLRHA}}$) and bending moment ($M_{x,\mathrm{NLRHA}}$) than X direction as observed in Fig. 12(a) and Fig. 12(b). For RSA procedure, shear force in X direction ($V_{x,\mathrm{RSA}}$) and in Y direction ($V_{y,\mathrm{RSA}}$) are similar because during design process, ASCE 7-10 requires scaling dynamic base shear determined by RSA to be at least equal to 85% of the static base shear computed by ELF procedure.

Shear demands from NLRHA were significantly larger than the design shear forces from RSA procedure along the height of core wall (Fig. 12(a)). The shear amplifications of core wall in coupled direction (V_x) were less than those in cantilever direction (V_y) and rather uniform along the height of core wall. Bending moment demands from NLRHA were much larger than the design bending moments from RSA procedure along the height of core wall (Fig. 12(b)). These large bending moments from NLRHA were mainly due to different axial load and flexural over-strength, as explained in base moment amplification in Section 6.1. The moment amplifications of core wall in coupled direction (M_y) were smaller than those in cantilever direction (M_x) because the flexural demands in coupled direction governed the design of core wall.

For story drift, ASCE 7-10 employs deflection amplification factor (C_d) not larger than the response modification factor (R) implying that inelastic story drifts computed by ASCE 7 procedure are always not larger than elastic story drifts. However, Fig. 12(c) shows that inelastic story drifts from NLRHA are larger than elastic story drifts from linear response history analysis (LRHA), while those computed by ASCE 7-10 procedure are the smallest. Therefore, estimating displacement and inter-story drifts by elastic value would be more accurate than those obtained by ASCE 7-10 procedure.

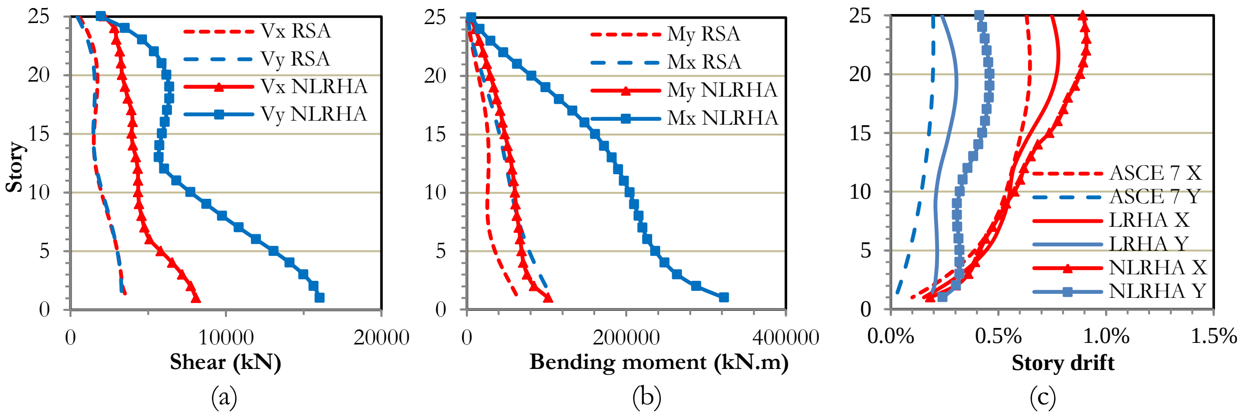

Fig. 12. Comparison of seismic demands obtained from RSA procedure and NLRHA: (a) shear force; (b) bending moment in core wall; and (c) story drift of the 25-story core wall located in Bangkok.

7. Accuracy of Previously Proposed Formulas for Estimating Shear Forces of RC Walls

The base shear amplification (BSA) compared here is defined as the ratio between base shear force from NLRHA (or the already-amplified design shear force from various codes and previous researcher's formula) and the design shear force from RSA procedure. The mean value (designated as NLRHA in Fig. 13 and Fig. 14) of BSA from NLRHA was presented along with mean plus and minus one standard deviation (mean±std.dev.) to show the variability of the shear amplification among different ground motions. To reasonably compare, the parameters required for each formula were taken the same as those used in this study. For EC8 [9], q was considered equal to R_{eff} (Table 5) and $\gamma_{Rd} M_{Rd} / M_{Ed}$ was taken the same as BFOS (Fig. 9). For Rejec et al. [6], $m(z)$ was taken the same as their proposed value. For Luu et al. [16], γ_w was taken equal to BFOS. Higher mode elastic (HME) method is included by modifying Priestley [5]'s equation only for inelastic first-mode shear. The inelastic first-mode shear force of HME, V_{1i}, was computed from $V_{1i} = \gamma_w V_{1Ei} / R_{eff}$ where γ_w was taken equal to BFOS and V_{1Ei} was elastic first-mode shear at level i.

In Bangkok, Rejec et al. [6]'s equation provided good agreement with BSA from NLRHA in cantilever direction of core wall (Fig. 13(b)), but it conservatively overestimated BSA in coupled direction (Fig. 13(a)). Rejec et al. [6]'s equation could well estimate the shear force along the height of core wall in cantilever direction (Fig. 14(b)), while it largely overestimated the shear force along the height of core wall in coupled direction (Fig. 14(a)). In Chiang Mai, Luu et al. [16]'s equation provided good agreement with BSA from NLRHA in both directions of core wall (Fig. 13(c) and Fig. 13(d)). It could well follow the trend of shear force along the height of core wall in both directions (Fig. 14(c) and Fig. 14(d)). Beside these two equations, EC8 [9]'s equation generally provided conservative results for both cantilever and coupled directions and both locations, Bangkok and Chiang Mai, with the exception that it slightly underestimated the base shear force in cantilever direction of 20- and 25-story core walls in Bangkok (Fig. 13(b)).

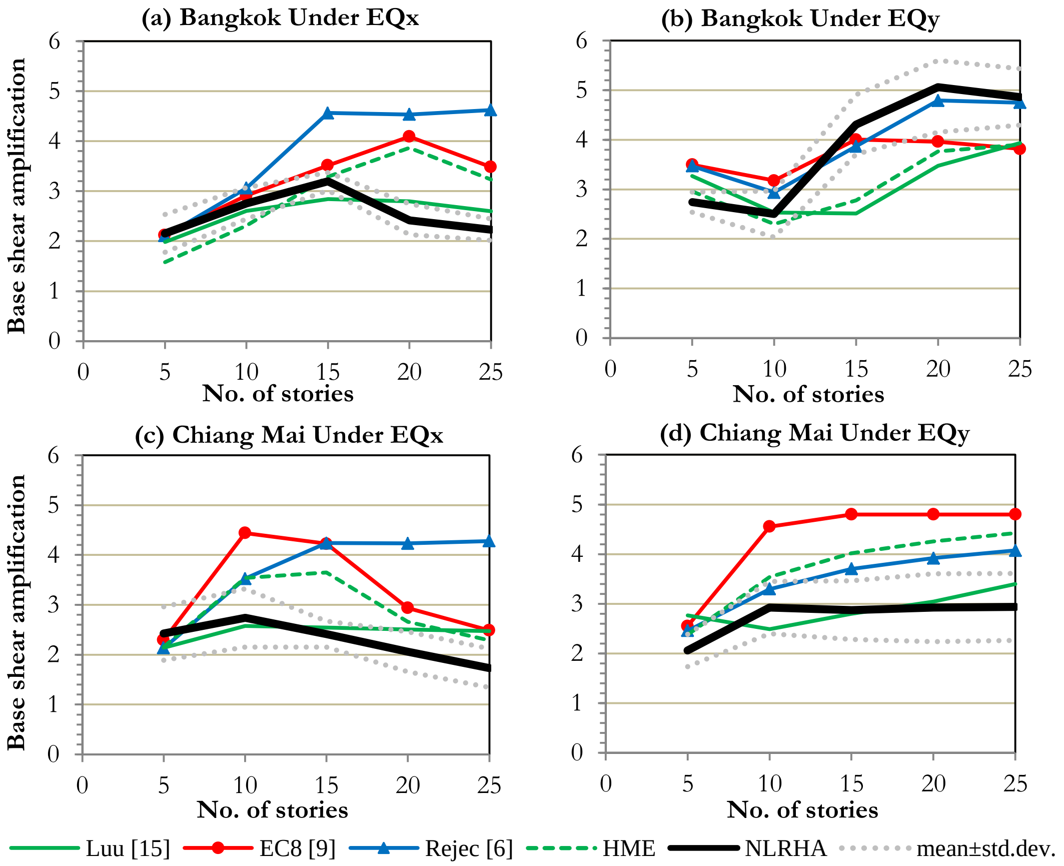

Fig. 13. Comparison of base shear amplifications from NLRHA in this study and previously proposed equations: (a) Bangkok under EQx; (b) Bangkok under EQy; (c) Chiang Mai under EQx; and (d) Chiang Mai under EQy.

8. Sensitivity of Shear Demands of RC Core Walls to Flexural Over-Strength

In practice, the structures are designed to have flexural strength much stronger than required by design. This extra strength is recognized as flexural over-strength. However, this flexural over-strength can increase shear force demands of the core wall. The sensitivity of shear demands of RC core walls to flexural over-strength are investigated in this section. The set of ground motions in Chiang Mai is used in this investigation. The following conditions were considered:

- Uniform vertical reinforcing ratio of core wall was used for all stories.
- Three different amounts of vertical reinforcement in core walls were used, which were equal to 50%, 100% and 150% of the reinforcing ratio at the base of core walls designed by RSA procedure as designated in Fig. 15 by U50%, U100% and U150%, respectively.
- Coupling beam strengths were kept the same as in core wall presented earlier.

Using uniform reinforcing ratio (U100%) along the height of core wall led to slightly increase of base shear amplifications of core walls comparing to non-uniform reinforcing ratio (N100%) which was the structures presented up to this section. Using U100% had little effect for taller buildings (20-and 25-story), as shown in Fig. 16.

The sensitivity of base shear amplification (BSA) to base flexural over-strength (BFOS) of core walls resulted from analysis of the buildings using U50%, U100%, and U150% as mention above was plotted in Fig. 17. BSA was increased with increasing of BFOS of core walls for all buildings in both directions. The significant influence of BFOS on BSA was indicated by the slope of BSA as summarized in Table 6. The larger slope means larger influence. The slopes of BSA in coupled direction (EQx) were larger than those in cantilever direction (EQy). This inferred that BFOS had less effect on BSA in cantilever direction. The slopes of BSA in 5- to 15-story core walls were larger than those in 20- to 25-story core walls indicating that BFOS had larger influence on BSA in shorter buildings than in taller buildings. Large value of BFOS is less important for tall buildings but it is more important for short buildings. The reason is that the first-mode shear contribution is dominant for short buildings but it is not for tall buildings. Therefore, for tall buildings, when the first-mode shear is multiplied with BFOS to get actual response after yielding, the influence is not as significant as for short buildings. As shown in Fig. 18, increasing of reinforcing ratios of core wall had only minor influence on shear force along the height of core wall in 25-story building (Fig. 18(c) and 18(d)) but this had larger effect on shear force along the height of core wall in 15-story building (Fig. 18(a) and 18(b)).

Table 6. Slope of BSA due to increasing of BFOS of core walls.

No. of Story	Slope of base shear amplification (%)	
	Under EQx	Under EQy
5	0.27	0.33
10	0.62	0.32
15	0.65	0.35
20	0.34	0.16
25	0.20	0.13

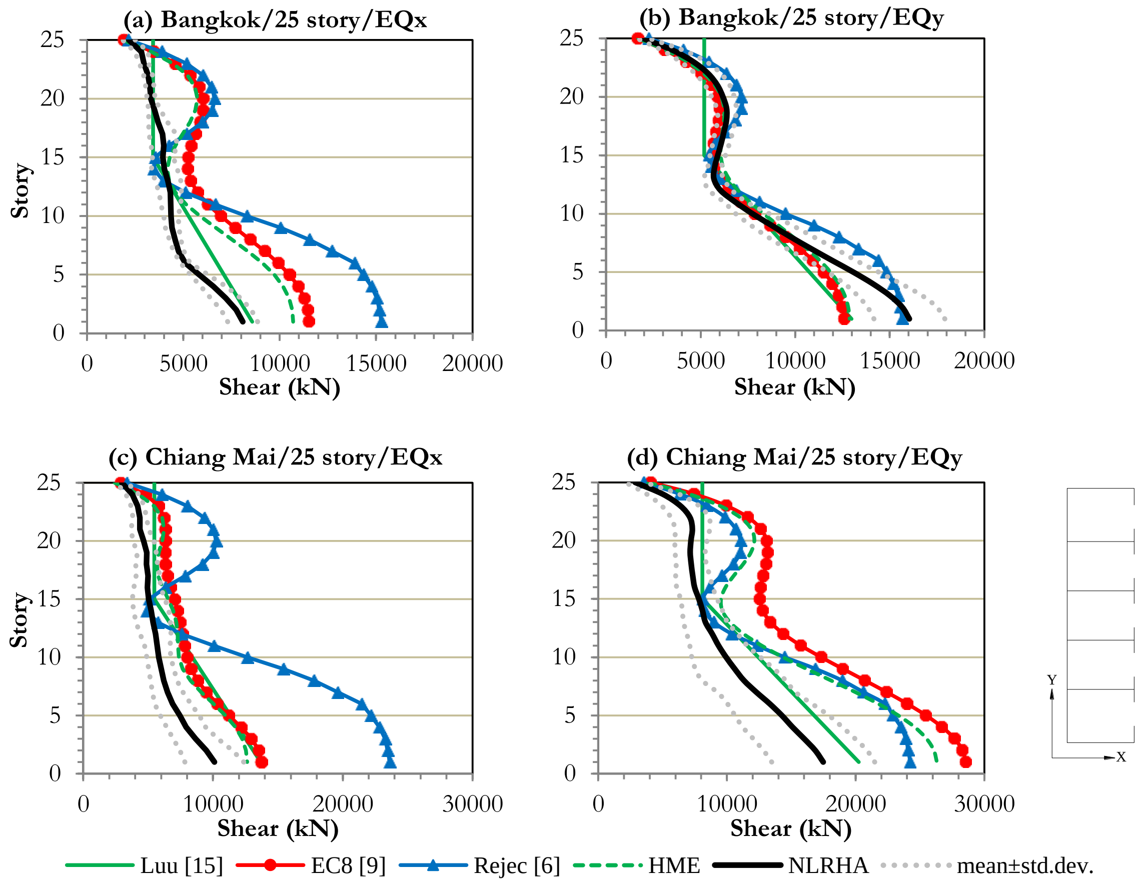

Fig. 14. Comparison of shear forces along the height of 25-story core wall from NLRHA in this study and previously proposed equations: (a) Bangkok under EQx; (b) Bangkok under EQy; (c) Chiang Mai under EQx; and (d) Chiang Mai under EQy.

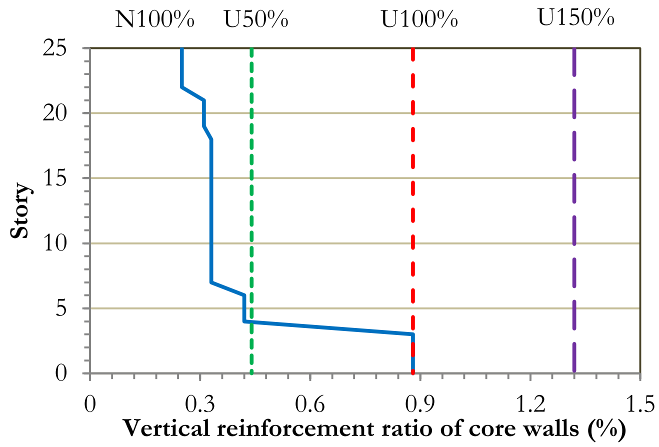

Fig. 15. Vertical reinforcement ratios of core walls in 25-story building.

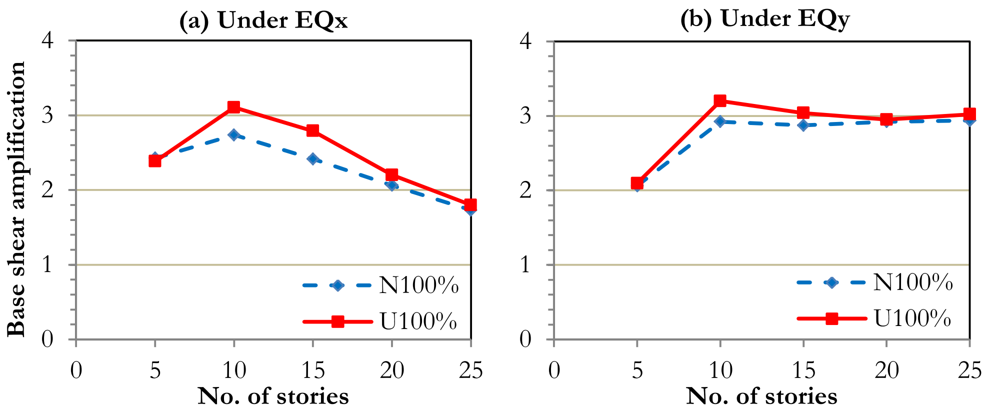

Fig. 16. Comparison of base shear amplifications from NLRHA by using non-uniform (N100%) and uniform reinforcement (U100%): (a) under EQx and (b) under EQy.

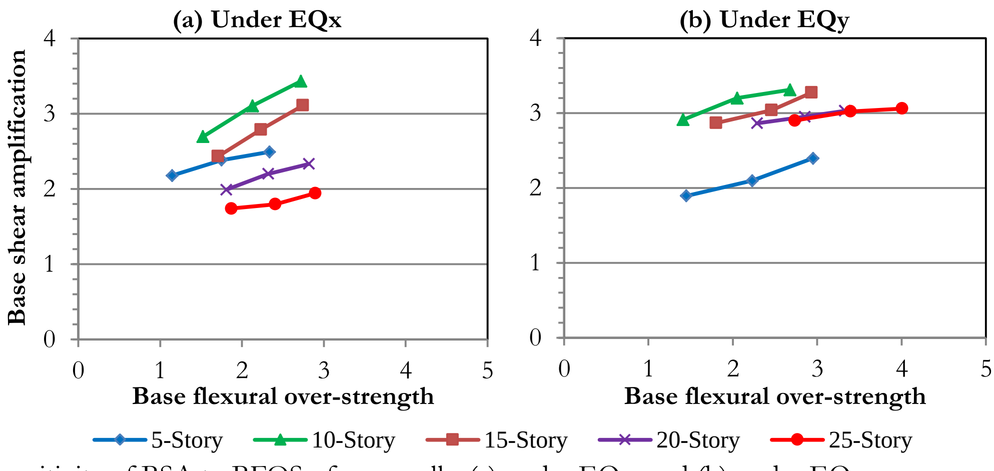

Fig. 17. Sensitivity of BSA to BFOS of core walls: (a) under EQx; and (b) under EQy.

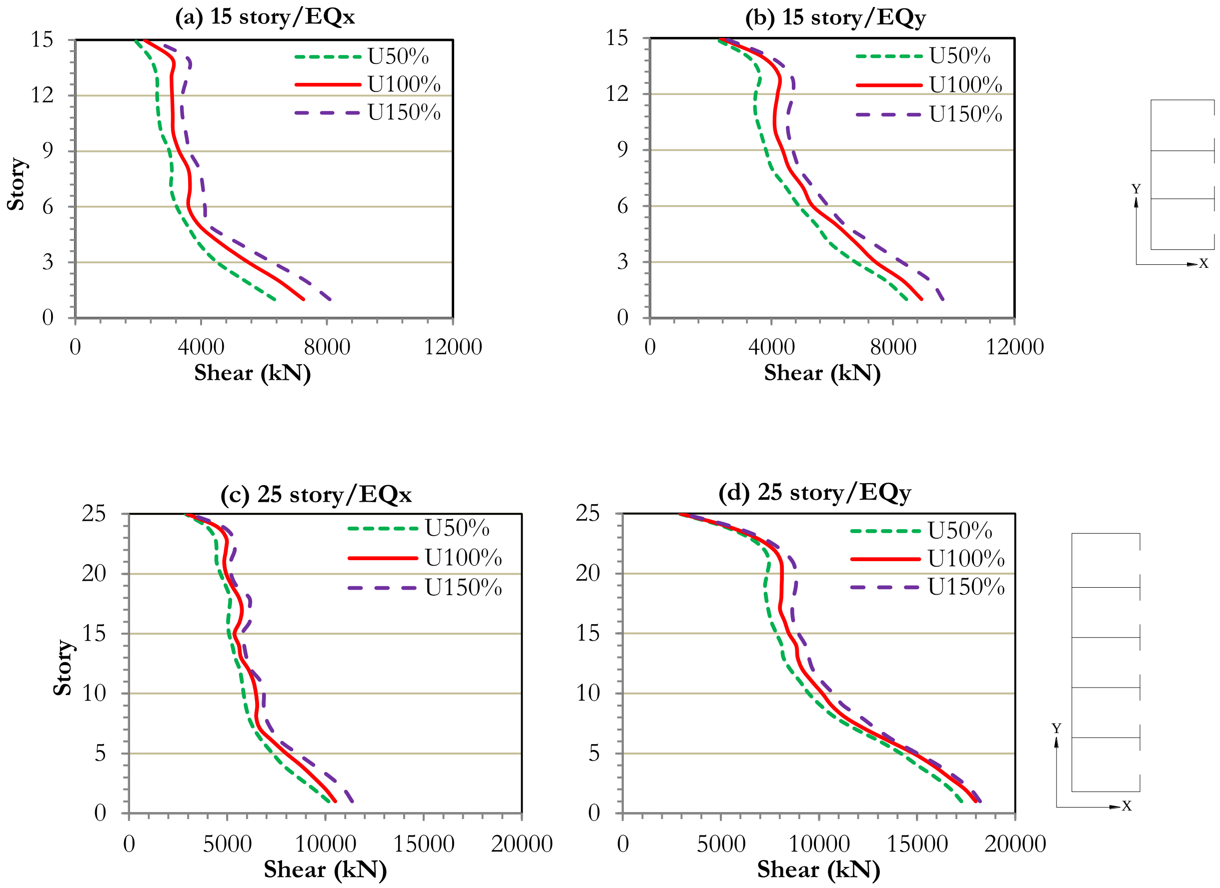

Fig. 18. Comparison of shear force along the height of core wall from NLRHA by using three different vertical reinforcement ratios of core wall: (a) 15-story under EQx; (b) 15-story under EQy; (c) 25-story under EQx; and (d) 25-story under EQy.

9. Effects of Elastic Wall in Upper Stories on Seismic Demands of RC Core Walls

All the results presented up to this section were based on the design concept that flexural strengths of the walls in every story were designed according to the flexural demands of the walls determined by RSA procedure. The walls can yield at any location along the height of the building. This design concept is named as distributed plastic hinge (DPH) model of the walls. However, in another design concept, the walls in upper stories are provided enough strength to prevent any yielding in upper stories and yielding is allowed to occur only at the base of the walls. This design concept is defined as single plastic hinge (SPH) model of the walls. The effects of designing the wall to behave elastically in upper stories on seismic demands of RC core wall were investigated.

For SPH model in this study, yielding could only occur at the first-story core wall and all coupling beams along the height of the building. The demands obtained from SPH model were compared with those from DPH model. The flexural strengths of 25-story core wall for SPH and DPH models were indicated in Fig. 19 as example of the difference between SPH and DPH modeling concepts.

Designing the walls in upper stories to remain elastic could lead to increase of base shear amplification (BSA) in coupled direction of core wall about 1.4 times comparing to BSA obtained from DPH design concept (Fig. 20(a)) but this had little influence on BSA in cantilever direction of core wall (Fig. 20(b)). SPH resulted in significantly larger shear forces than DPH at upper stories in both directions of core wall (Fig. 21).

SPH design concept caused significantly large bending moment at mid-height of core wall in both directions (Fig. 22). These large bending moments at the mid-height were closed to the bending moments at the base of core wall. Hence, designing the mid-height walls to behave elastically required excessive vertical reinforcement. At the base of core wall, there were not much difference of bending moments computed from SPH and DPH because core walls could easily yield, and then bending moment demands were limited by flexural strengths of core wall.

SPH design concept resulted in decreasing of story drifts at upper stories (Fig. 23). The roof drifts from SPH could reduce up to about 30% comparing to those from DPH. While at lower stories near the base, story drifts from SPH were slightly larger than those from DPH. These kinds of differences between story drifts from SPH and DPH came from the fact that elastic story drifts were smaller than inelastic story drifts as discussed in Section 6.2.

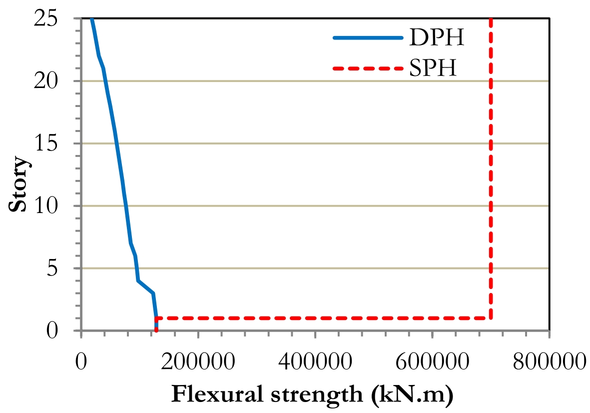

Fig. 19. Flexural strength of 25-story core wall in DPH and SPH design concepts.

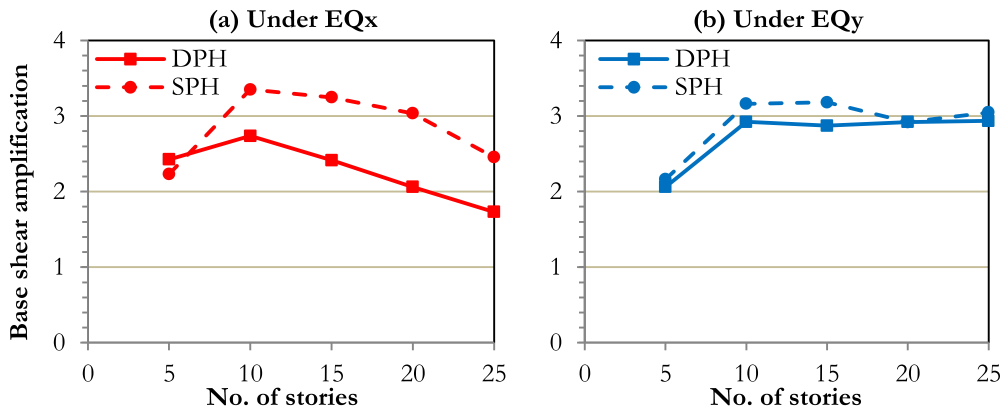

Fig. 20. Comparison of base shear amplifications of core walls obtained from NLRHA for SPH and DPH design concepts: (a) under EQx; and (b) under EQy.

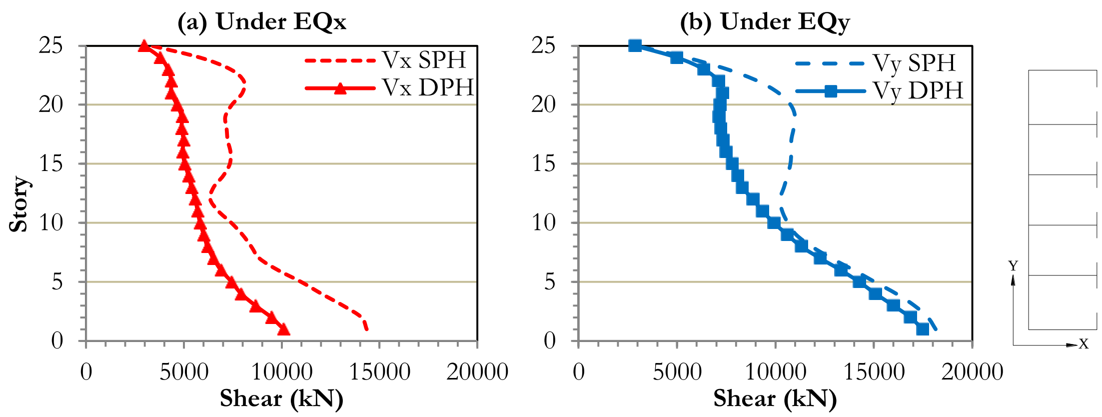

DOI:10.4186/ej.2017.21.2.151

Fig. 21. Comparison of shear demands of 25-story core wall obtained from NLRHA for SPH and DPH design concepts: (a) under EQx; and (b) under EQy.

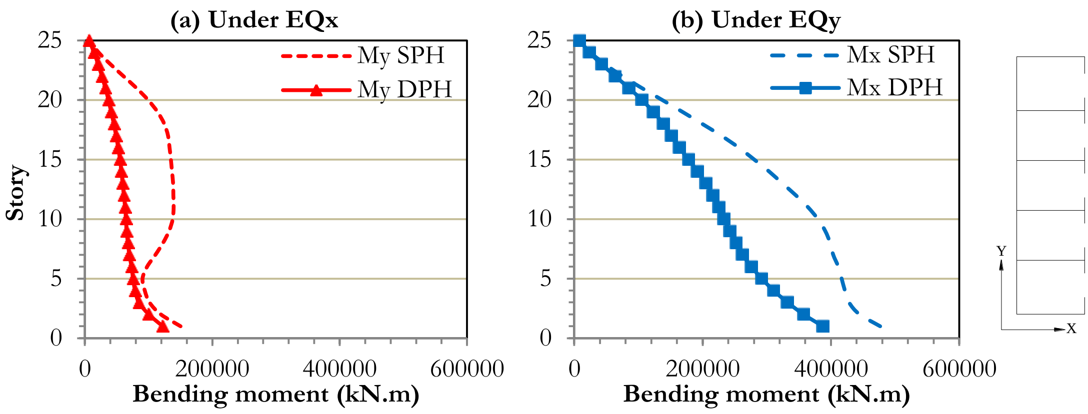

Fig. 22. Comparison of bending moment demands of 25-story core wall obtained from NLRHA for SPH and DPH design concepts: (a) under EQx; and (b) under EQy.

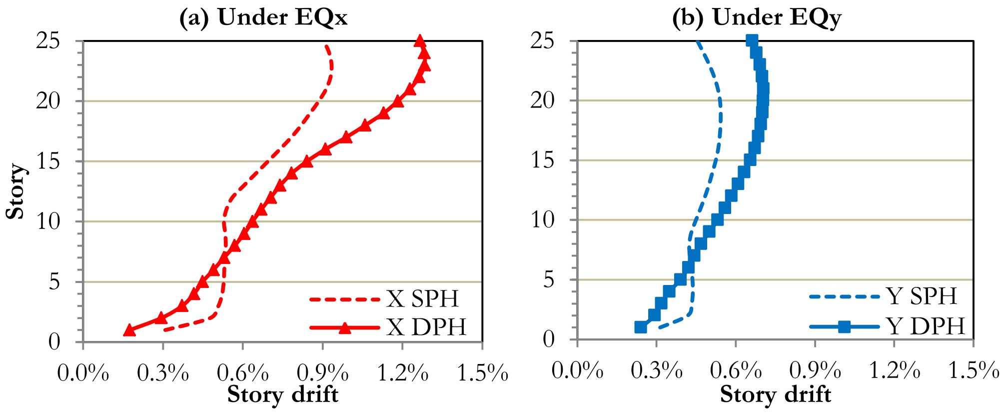

Fig. 23. Comparison of story drifts of 25-story core wall obtained from NLRHA for SPH and DPH design concepts: (a) under EQx; and (b) under EQy.

10. Conclusions

This study has evaluated the seismic demands of RC core walls obtained from response spectrum analysis (RSA) procedure in ASCE 7-10 by using nonlinear response history analysis (NLRHA). RC split core walls in five buildings varying from 5 to 25 stories, which were subjected to ground motions in two different cities, Bangkok and Chiang Mai in Thailand, were employed. Two directions of core wall whose behaviors are different as it behaves like cantilever wall in Y direction and coupled wall in X direction were studied. The accuracy of various codes and previously proposed formulas for estimating the design shear force of RC wall was evaluated. The following conclusions could be drawn:

1. The shear demands in core walls determined by NLRHA are significantly larger than the design shear forces used in RSA procedure. In cantilever-wall direction, the base shear amplification (BSA) of core walls could be as high as two to five in Bangkok and two to three in Chiang Mai, while in coupled-wall direction, they are relatively lower.
2. Different building locations having different spectrum shapes can lead to different shear amplifications. Hence, an empirical equation cannot be applied to every location. In Bangkok, it is found that Rejec et al. [6]'s equation could well estimate shear demands in cantilever direction of core walls but it significantly overestimates in coupled direction of core walls. In Chiang Mai, Luu et al. [16]'s equation could provide good estimation of shear forces in both directions of core walls. Beside these two equations, the shear magnification factor equation in EC8 is found acceptable to

be adopted to multiply with shear force from RSA procedure before using it as design shear force of RC core wall in both Bangkok and Chiang Mai. EC8's equation generally provides conservative results with the exception that it slightly underestimates the base shear force in core-wall buildings of 20 and 25 stories.

3. Flexural over-strength of core walls inherent in the design process can lead to increase of shear demands in both direction of core walls. This has less influence on shear demands of core walls in cantilever direction comparing to those in coupled direction. Large flexural over-strength is less important to increase shear demands of core walls in tall buildings but it is significant to increase shear demands of core walls in short buildings.
4. Single plastic hinge (SPH) design concept, which prevents yielding to occur in upper stories of core walls, can lead to increase of base shear amplification (BSA) in coupled direction of core walls about 1.4 times those from distributed plastic hinge (DPH) design concept, which allows yielding to occur at any location throughout the height of core walls. This has little influence on BSA in cantilever direction of core walls. Designing the core walls in upper stories to behave elastically requires excessive amounts of vertical reinforcement because bending moments of core walls at mid-height are closed to the bending moments at the base of core walls.

Acknowledgement

The authors gratefully acknowledge the financial support of JICA through the ASEAN University Network/Southeast Asia Engineering Education Development Network (AUN/SEED-Net) program. The helpful suggestions for this study provided by Assoc. Prof. Anil C. Wijeyewickrema at Tokyo Institute of Technology are highly appreciated.

References

[1] American Society of Civil Engineers, *Minimum design loads for buildings and other structures*, ASCE standard ASCE/SEI 7-10, Reston, 2010.

[2] V. Calugaru and M. Panagiotou, "Response of tall cantilever wall buildings to strong pulse type seismic excitation," *Earthquake Engineering & Structural Dynamics*, vol. 41, no. 9, pp. 1301-1318, 2012.

[3] J. Eibl and E. Keintzel, "Seismic shear forces in RC cantilever shear walls," in *9th world conference on earthquake engineering*, Tokyo-Kyoto, Japan, 1988.

[4] A. Munir and P. Warnitchai, "The cause of unproportionately large higher mode contributions in the inelastic seismic responses of high-rise core-wall buildings," *Earthquake Engineering & Structural Dynamics*, vol. 41, no. 15, pp. 2195-2214, 2012.

[5] M. J. N. Priestley, "Does capacity design do the job? An examination of higher mode effects in cantilever walls," *Bulletin of the New Zealand Society for Earthquake Engineering*, vol. 36, no. 4, pp. 276-292, 2003.

[6] K. Rejec, T. Isaković, and M. Fischinger, "Seismic shear force magnification in RC cantilever structural walls, designed according to Eurocode 8," *Bulletin of Earthquake Engineering*, vol. 10, no. 2, pp. 567-586, 2012.

[7] NBCC, *National building code of Canada*, Commission on Building and Fire Codes, National Research Council of Canada, 2010.

[8] CSA, *Design of concrete structures*, CSA standard A23.3-04, Canadian Standard Association, 2004.

[9] CEN, *Eurocode 8: Design of structures for earthquake resistance-Part 1: General rules, seismic actions and rules for buildings*, Brussels, 2004.

[10] NZS, *NZS 3101: part 2: Commentary on the design of concrete structures*, New Zealand Standards, Wellington, 2006.

[11] A. Rutenberg, "Seismic shear forces on RC walls: review and bibliography," *Bulletin of Earthquake Engineering*, vol. 11, no. 5, pp. 1727-1751, 2013.

[12] K. Leng, C. Chintanapakdee, and T. Hayashikawa, "Seismic shear forces in shear walls of a medium-rise building designed by response spectrum analysis," *Engineering Journal*, vol. 18, no. 4, pp. 73-95, 2014.

[13] R. W. G. Blakeley, R. C. Cooney, and L. M. Megget, "Seismic shear loading at flexural capacity in cantilever wall structures," *Bulletin of the New Zealand Society for Earthquake Engineering*, vol. 8, no., pp. 278–290, 1975.

DOI:10.4186/ej.2017.21.2.151

[14] A. Rutenberg and E. Nsieri, "The seismic shear demand in ductile cantilever wall systems and the EC8 provisions," *Bulletin of Earthquake Engineering*, vol. 4, no. 1, pp. 1-21, 2006.

[15] Y. Boivin and P. Paultre, "Seismic force demand on ductile reinforced concrete shear walls subjected to western North American ground motions: Part 2 - new capacity design methods," *Canadian Journal of Civil Engineering*, vol. 39, no. 7, pp. 738-750, 2012.

[16] H. Luu, P. Léger, and R. Tremblay, "Seismic demand of moderately ductile reinforced concrete shear walls subjected to high-frequency ground motions," *Canadian Journal of Civil Engineering*, vol. 41, no. 2, pp. 125-135, 2014.

[17] P. Adebar, J. Mutrie, R. DeVall, and D. Mitchell, "Seismic design of concrete buildings: The 2015 Canadian Building Code," in *Proceeding of 10th National Conference on Earthquake Engineering*, 2014.

[18] Computers and Structures, *ETABS, Integrated Building Design Software, Version 13.2.0*. Berkeley, CA, 2013.

[19] ACI 318 Committee, "Building code requirements for structural concrete and commentary," ACI 318-11. American Concrete Institute, 2011.

[20] Computers and Structures, *PERFORM-3D, Nonlinear Analysis and Performance Assessment of 3D Structures, Version 5.0.0*. Berkeley, CA, 2011.

[21] G. Powell, *Detailed Example of a Tall Shear Wall Building Using CSI's Perform 3D Nonlinear Dynamic Analysis*. Berkeley, CA: Computers and Structures Inc., 2007.

[22] Applied Technology Council, "Modeling and acceptance criteria for seismic design and analysis of tall buildings," PEER/ATC-72-1, 2010.

[23] J. B. Mander, M. J. Priestley, and R. Park, "Theoretical stress-strain model for confined concrete," *Journal of Structural Engineering*, vol. 114, no. 8, pp. 1804-1826, 1988.

[24] M. J. N. Priestley, G. M. Calvi, and M. J. Kowalsky, *Displacement-Based Seismic Design of Structures*. Pavia: IUSS Press, 2007.

[25] J. P. Moehle, Y. Bozorgnia, N. Jayaram, P. Jones, M. Rahnama, N. Shome, Z. Tuna, J. W. Wallace, T. Y. Yang, and F. Zareian, "Case studies of the seismic performance of tall buildings designed by alternative means," Task 12 Report for the Tall Buildings Initiative, PEER-2011/05, Pacific Earthquake Engineering Research Center, University of California, Berkeley, CA, 2011.

[26] D. A. B. Naish, A. Fry, R. Klemencic, and J. Wallace, "Reinforced concrete coupling beams—Part II: Modeling," *ACI Structural Journal*, vol. 110, no. 06, 2013.

[27] C. Palasri and A. Ruangrassamee, "Probabilistic seismic hazard maps of Thailand," *Journal of Earthquake and Tsunami*, vol. 4, no. 04, pp. 369-386, 2010.

[28] EduPro Civil System, *ProShake Ground Response Analysis Program, User's Manual, Version 1.1, Inc.* Redmond, Washington, 2004.